Human CAR T cells with cell-intrinsic PD-1 checkpoint blockade resist tumor-mediated inhibition

Leonid Cherkassky,[1,2] Aurore Morello,[1,2] Jonathan Villena-Vargas,[1,2] Yang Feng,[3] Dimiter S. Dimitrov,[3] David R. Jones,[2] Michel Sadelain,[1] and Prasad S. Adusumilli[1,2]

[1]Center for Cell Engineering and [2]Thoracic Service, Department of Surgery, Memorial Sloan Kettering Cancer Center, New York, New York, USA. [3]Protein Interactions Section, Laboratory of Experimental Immunology, Cancer and Inflammation Program, Center for Cancer Research, National Cancer Institute, NIH, Frederick, Maryland, USA.

Following immune attack, solid tumors upregulate coinhibitory ligands that bind to inhibitory receptors on T cells. This adaptive resistance compromises the efficacy of chimeric antigen receptor (CAR) T cell therapies, which redirect T cells to solid tumors. Here, we investigated whether programmed death-1–mediated (PD-1–mediated) T cell exhaustion affects mesothelin-targeted CAR T cells and explored cell-intrinsic strategies to overcome inhibition of CAR T cells. Using an orthotopic mouse model of pleural mesothelioma, we determined that relatively high doses of both CD28- and 4-1BB–based second-generation CAR T cells achieved tumor eradication. CAR-mediated CD28 and 4-1BB costimulation resulted in similar levels of T cell persistence in animals treated with low T cell doses; however, PD-1 upregulation within the tumor microenvironment inhibited T cell function. At lower doses, 4-1BB CAR T cells retained their cytotoxic and cytokine secretion functions longer than CD28 CAR T cells. The prolonged function of 4-1BB CAR T cells correlated with improved survival. PD-1/PD-1 ligand [PD-L1] pathway interference, through PD-1 antibody checkpoint blockade, cell-intrinsic PD-1 shRNA blockade, or a PD-1 dominant negative receptor, restored the effector function of CD28 CAR T cells. These findings provide mechanistic insights into human CAR T cell exhaustion in solid tumors and suggest that PD-1/PD-L1 blockade may be an effective strategy for improving the potency of CAR T cell therapies.

Introduction

Chimeric antigen receptors (CARs) are synthetic receptors that retarget T cells to tumor surface antigens (1, 2). First-generation receptors typically link an antibody-derived tumor-binding element to either CD3ζ or Fc receptor signaling domains to trigger T cell activation. The advent of second-generation CARs, which combine activating and costimulatory signaling domains, has led to encouraging results in patients with chemorefractory B cell malignancies (3–7). The translation of this clinical success to solid tumors will require overcoming multiple obstacles, which include achieving sufficient T cell infiltration into tumors and the prevention of tumor immune escape. To overcome the limitations of tumor infiltration and delayed activation observed with systemic T cell administration, we recently demonstrated the merits of regional administration of mesothelin-specific (MSLN-specific) CAR T cells in a clinically relevant model of pleural mesothelioma (8). MSLN is a tumor-associated cell-surface antigen, which we selected on the basis of its overexpression in several cancers and our observations of its association with tumor aggressiveness in mesothelioma and lung and breast cancer patients (9–17). Regional administration of MSLN-targeted CAR T cells establishes long-term systemic immunosurveillance requiring 30-fold lower doses than intravenous administration (8). Aware of potential low T cell infiltration in solid tumors, we investigated CAR T cell efficacy when administered at very low doses.

To eliminate tumor cells, T cells must not only persist, but sustain cytolytic and proliferative function, eluding the inhibitory signals encountered in the tumor microenvironment. The success of second-generation CAR T cells has been attributed to the enhanced T cell persistence afforded by costimulatory signaling domains, such as CD28 and the TNF receptor 4-1BB. However, T cells naturally undergo activation-induced upregulation of coinhibitory pathways, which may limit the antitumor immune response. Programmed death-1 (PD-1), cytotoxic T-lymphocyte–associated protein 4 (CTLA-4), and other coinhibitory receptors are upregulated in T cells following antigen encounter, while tumor cells augment the expression of coinhibitory ligands such as PD-1 ligand (PD-L1) following exposure to T cell–secreted Th1 cytokines (18–20). The success of antibody therapy targeting immune checkpoints such as PD-1 and CTLA-4 underscores the therapeutic potential of counteracting immune inhibition (21–23). However, the success of antibody-mediated checkpoint blockade requires a relatively high mutation burden and the presence of infiltrating T cells (24–26). Adoptive transfer of tumor-targeted T cells may thus fill the void in patients with less immunogenic or "noninflamed" tumors. As adoptively transferred T cells are themselves susceptible to immunoinhibition, strategies that combine adoptive T cell therapy with checkpoint antibody blockade have been investigated using mouse T cells (27–29). Antibody-mediated checkpoint blockade effectively provides reversal of immunoinhibition in a systemic fashion that may result in auto-

▶ Related Commentary: p. 2795

Authorship note: L. Cherkassky and A. Morello contributed equally to this work.
Conflict of interest: The authors have declared that no conflict of interest exists.
Submitted: June 3, 2015; **Accepted:** May 19, 2016.
Reference information: *J Clin Invest*. 2016;126(8):3130–3144. doi:10.1172/JCI83092.

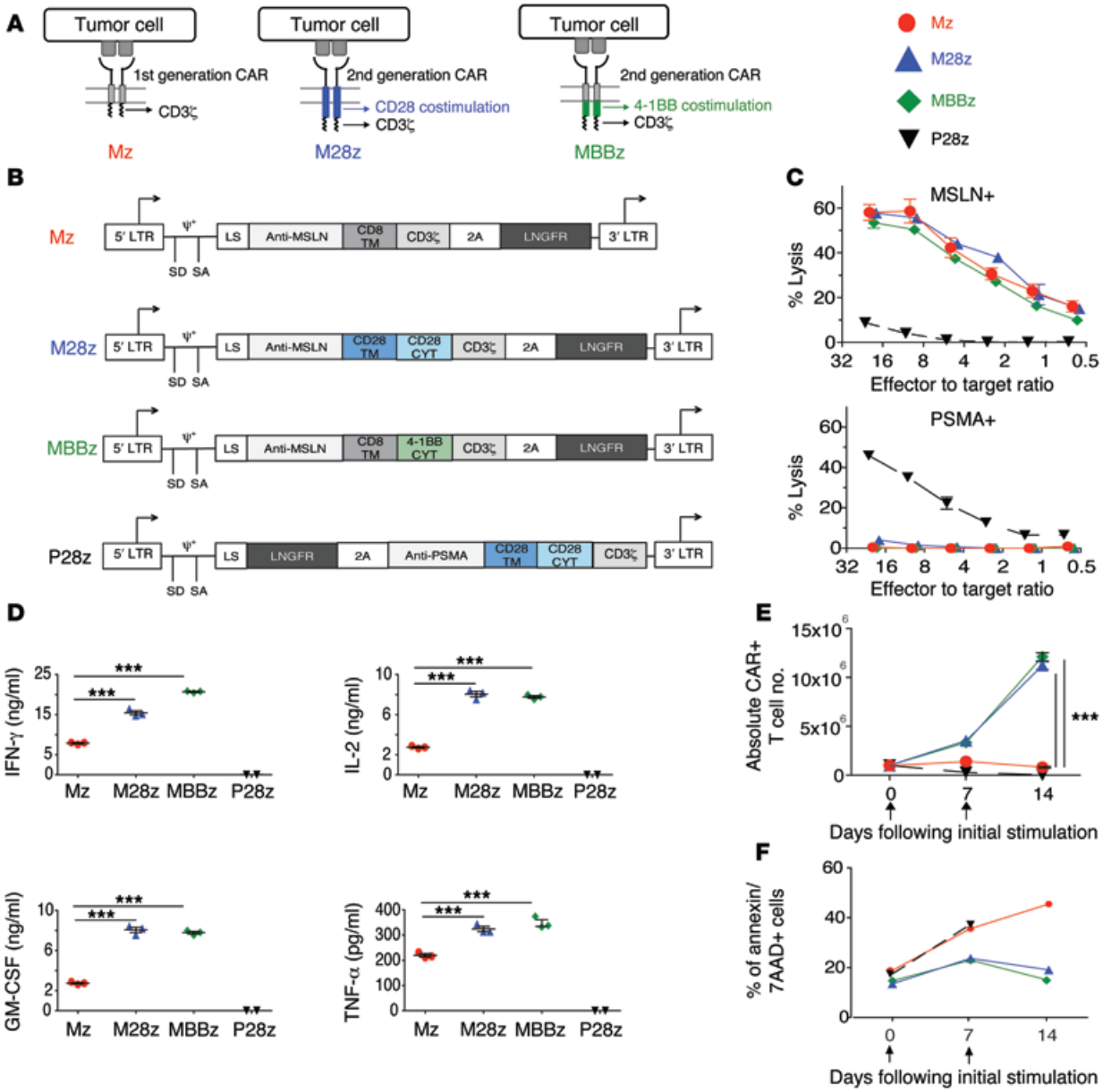

Figure 1. CARs with CD28 or 4-1BB costimulation exhibit similar cytolytic functions, effector cytokine secretion, and proliferation in vitro upon initial antigen stimulation. (**A**) First- and second-generation CARs. (**B**) MSLN–targeted CARs contain the CD3ζ endodomain either alone (Mz, first-generation CAR) or in combination with the CD28 (M28z) or 4-1BB (MBBz) costimulatory domain (second-generation CAR). PSMA-directed CARs with CD28 costimulation (P28z) as well as PSMA-expressing targets (PSMA$^+$) are included in experiments as negative controls. CYT, cytoplasmic domain; LS, leader sequence; LTR, long terminal repeat; SA, splice acceptor; SD, splice donor; TM, transmembrane. (**C**–**E**) Antigen-specific effector functions of CAR-transduced T cells. (**C**) Lysis of MSLN-expressing targets (MSLN$^+$), but not PSMA$^+$ targets, as measured by chromium-release assays. (**D**) 4-1BB and CD28 costimulations enhance cytokine secretion, as assessed by Luminex assay, after coculture of CAR T cells with MSLN$^+$ cells. (**E**) M28z and MBBz CARs facilitate robust T cell accumulation after stimulation with MSLN$^+$ cells. (**F**) 4-1BB and CD28 costimulations decrease the rate of apoptosis as assessed by annexin V/7-AAD$^+$ staining every 7 days after coculture with MSLN$^+$ target. (**D** and **E**) ***$P < 0.001$, comparing costimulated CAR T cells (M28z or MBBz) with the first-generation receptor (Mz), by Student's *t* test; significance was determined using the Sidak-Bonferonni correction for multiple comparisons. Data are representative of at least 3 independent experiments and represent the mean ± SEM (**C** and **E**) of 3 replicates or are plotted as individual points.

immune responses. In contrast, T cell engineering allows one to transduce receptors that selectively counteract tumor-mediated inhibition in targeted T cells.

In this report, we establish that human CAR T cells are subject to inhibition of their cytolytic and cytokine secretion functions upon repeated antigen encounter in vivo. We document the differing abilities of different costimulatory strategies (4-1BB vs. CD28) to withstand repeated antigen stimulation–induced exhaustion and analyzed one of the mechanisms of tolerance (i.e., PD-1 receptor/PD-L1 engagement). We demonstrate that PD-1–mediated CAR T cell exhaustion can be reversed by PD-1 antibody checkpoint blockade. We further describe a PD-1 dominant negative receptor (DNR) that, when cotransduced with a second-generation CAR, mediates enhanced T cell functional persistence

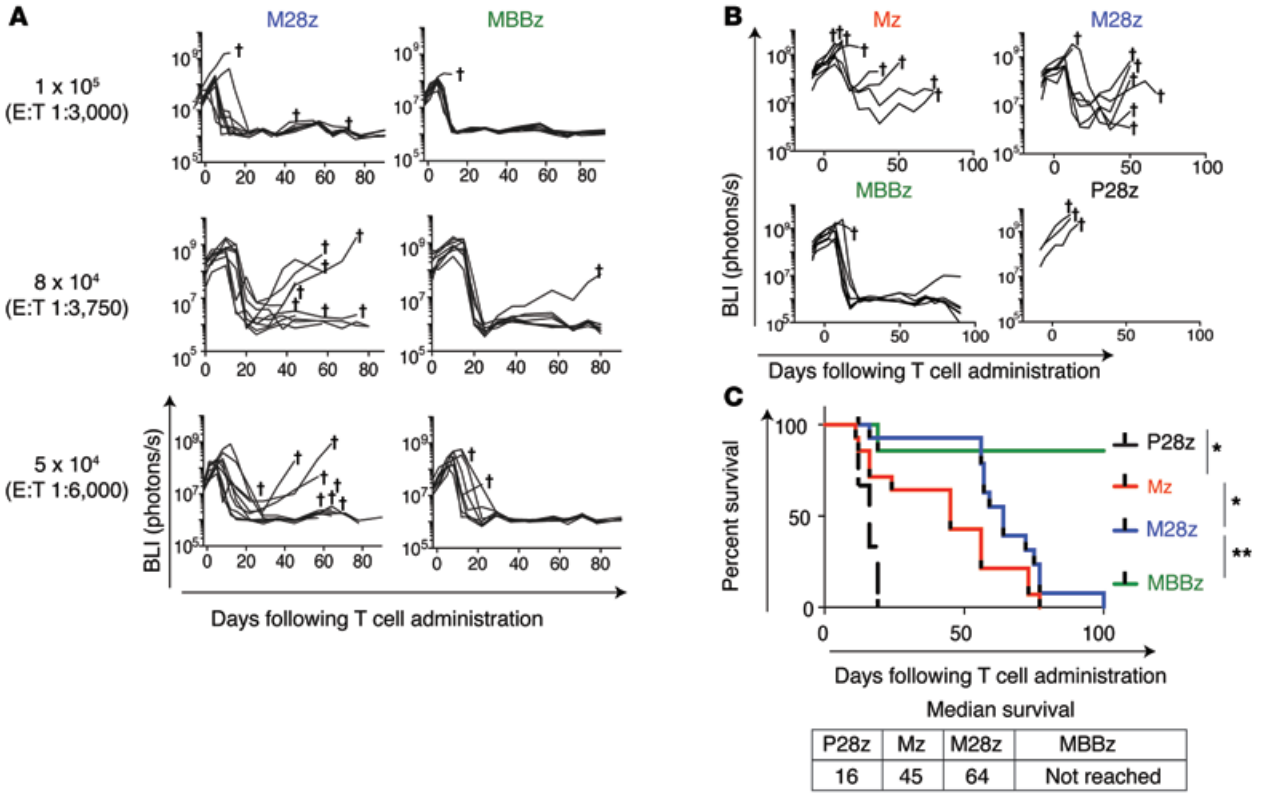

Figure 2. Mice treated with M28z and MBBz CAR T cells demonstrate tumor eradication at a higher dose, whereas treatment with lower doses results in higher rate of tumor relapse with M28z. (**A**) In vivo BLI was used to monitor tumor burden (ffLuc$^+$MSLN$^+$) in NOD/SCID/γ_c^{null} mice. Mice with established pleural tumor were treated with a single dose of 1×10^5 (E:T 1:3,000), 8×10^4 (E:T1:3,750), or 5×10^4 (E:T 1:6,000) M28z or MBBz CAR T cells. Daggers indicate the deaths of mice. For **A** and **B**, 2 similar experiments with the same donor are combined for the illustration. n = 7–9 mice for each group treated with MSLN-targeted CAR T cells. (**B**) Mice were treated with 4×10^4 CAR T cells (E:T 1:7,500). The first generation Mz CAR and negative control P28z are included. (**C**) Kaplan-Meier survival analysis comparing the in vivo efficacy of intrapleural administration of 4×10^4 Mz (n = 13, red), M28z (n = 15, blue), MBBz (n = 8, green), and P28z (n = 3, black) CAR T cells. Two independent experiments performed under similar conditions were combined. Median survival in days following T cell administration. The survival curve was analyzed using the log-rank test. *$P < 0.05$; **$P < 0.01$. All data are representative of multiple experiments performed with multiple donors.

as well as T cell resistance to tumor-mediated T cell inhibition. Our results demonstrate the benefit of simultaneously providing costimulation and checkpoint blockade to counteract tumor-mediated T cell inhibition in MSLN-expressing solid tumors.

Results

CARs with CD28 or 4-1BB costimulation exhibit equivalent effector cytokine secretion and proliferation in vitro upon initial antigen stimulation. We constructed 3 CARs that incorporated a human MSLN-specific scFv (30) and either CD3ζ, CD28/CD3ζ, or 4-1BB/CD3ζ signaling domains (Mz, M28z, MBBz) (Figure 1, A and B). The P28z CAR, which is specific for prostate-specific membrane antigen (PSMA), served as a negative effector to control for alloreactivity and xenoreactivity. Both CD4$^+$ and CD8$^+$ human peripheral blood T lymphocytes were effectively transduced using the SFG-retroviral vector (50%–70% transduction) (Supplemental Figure 1; supplemental material available online with this article; doi:10.1172/JCI83092DS1). MSLN-transduced MSTO-211H (MSLN$^+$) cells and PSMA-transduced EL-4 mouse lymphoma (MSLN$^-$) cells served as MSLN-positive and -negative targets. Mz-, M28z-, and MBBz-transduced T cells demonstrated similar MSLN-specific lysis in vitro (Figure 1C). P28z CAR T cells did not lyse MSTO MSLN$^+$ cells, and MSLN-targeted CARs did not lyse EL4 PSMA$^+$ cells — demonstrating that lysis is antigen specific. Validating the functionality of costimulatory signaling (31), M28z and MBBz CAR T cells secreted 2- to 15-fold higher levels of Th1 cytokines (Figure 1D) and achieved 8- to 14-fold greater T cell accumulation upon repeated exposure to MSLN$^+$ cells when compared with Mz in the absence of exogenous IL-2 (Figure 1E). Furthermore, CAR$^+$ T cells expressing costimulatory molecules (M28z and MBBz) exhibited lower rates of cell death compared with Mz and P28z on day 7 and day 14. No significant difference in cell death was observed between M28z and MBBz (Figure 1F). Having established antigen specificity and validated the functionality of costimulatory signaling domains, we proceeded to evaluate the therapeutic potential of MSLN-targeted CAR T cells in mice bearing established pleural tumors.

M28z is more prone to allowing tumor relapse than MBBz. In an orthotopic model of malignant pleural mesothelioma (MPM) previously established by our laboratory (15, 32–34), serial bioluminescence imaging (BLI) with firefly-luciferase–transduced (ffLuc-transduced) MSTO-211H cells was used to confirm the establishment of tumor, to equalize tumor burden across intervention groups before the initiation of T cell therapy, and to measure the response to thera-

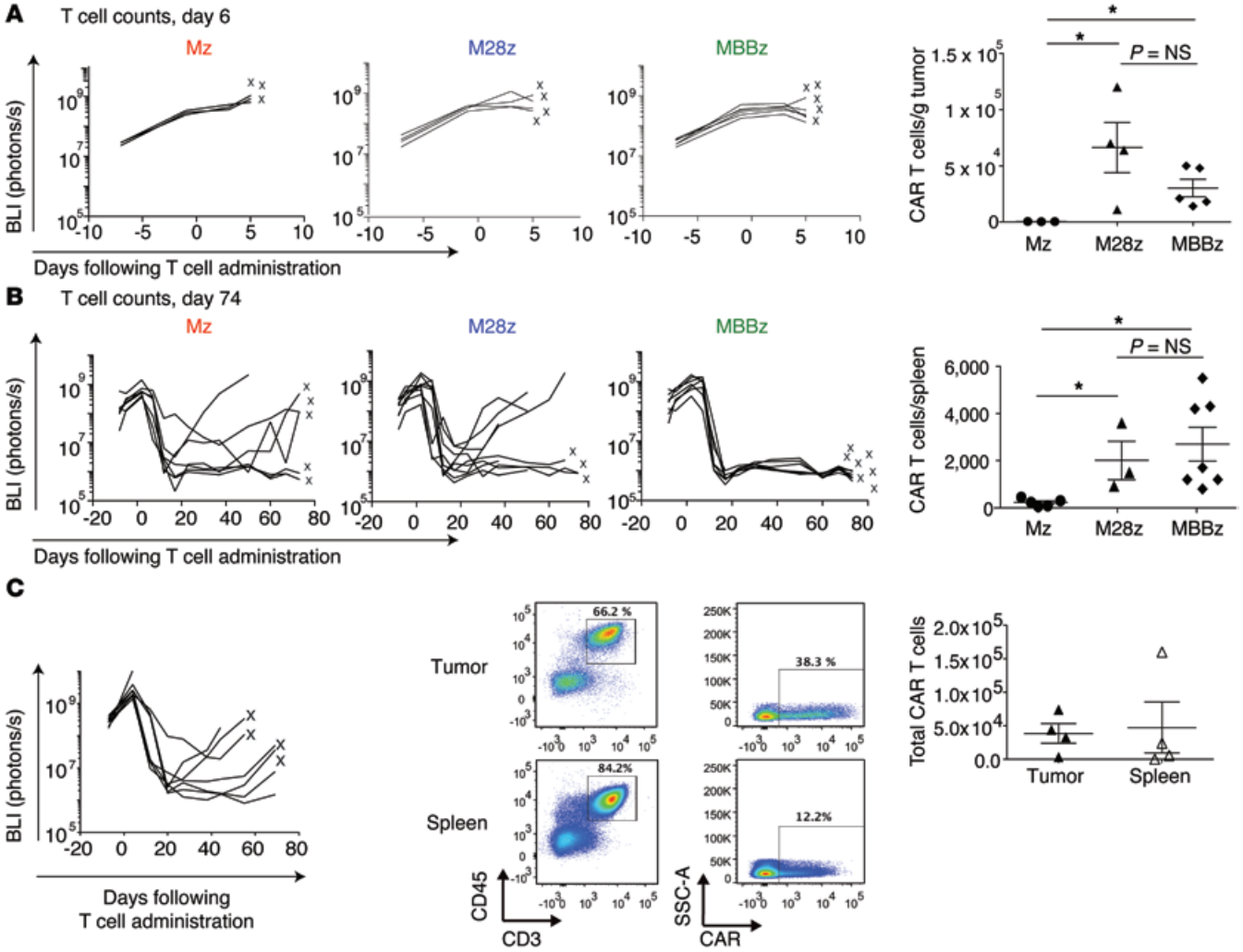

Figure 3. M28z- and MBBz-treated mice demonstrate similar early and long-term CAR T cell accumulation, and M28z-treated mice with progressing tumors contain persisting CAR T cells. (**A**) CD28 and 4-1BB costimulation enhance intratumoral CAR T cell accumulation to equal extents. The left panels show the results of tumor BLI after administration of a single dose of 8×10^4 CAR T cells. After 6 days, T cells were harvested from the tumor; x's denote mice whose T cell counts are represented as data points. The right panel shows absolute CAR T cells per gram of tumor tissue. $^*P < 0.05$. Student's *t* tests were performed, and statistical significance was determined using the Sidak-Bonferonni correction for multiple comparisons. (**B**) CD28 and 4-1BB costimulation enhance CAR T cell persistence, as measured in the spleen, to equal extents. Absolute CAR T cells per spleen are shown 74 days after intrapleural administration of CAR T cells (8×10^4). The left panels show the results of tumor BLI; x's denote mice whose T cell counts are represented as data points. $^*P < 0.05$. Student's *t* tests were performed, and statistical significance was determined using the Sidak-Bonferonni correction for multiple comparisons. (**C**) Mice treated with a low dose of M28z T cells (4×10^4) display tumor recurrence with persisting CAR T cells in the spleen and tumor. The left panel shows the results of tumor BLI. Spleen and tumor from mice denoted by an x were harvested and used for FACS analysis (middle panel) and T cell quantification (right panel). Data are representative of multiple tested mice of at least 3 independent experiments.

py. Both M28z and MBBz CAR T cells intrapleurally administered at a single dose of 1×10^5 (effector to target [E:T] ratio of 1:3,000, estimated from tumor burden quantification) (33) were able to eradicate established pleural tumors in the majority of mice (Figure 2A). Since our goal in this study was to investigate the effect of tumor-induced immunoinhibition on T cell exhaustion, we administered CAR T cells to mice bearing established pleural tumors at successively lower doses. We hypothesized that at these lower doses, T cells would be especially susceptible to exhaustion, as they must retain function upon repeated antigen encounters in order to eliminate tumor. It is at these lower doses that we began to see tumor relapse, especially within the M28z cohort (Figure 2A). At the lowest dose tested of 4×10^4 (E:T, 1:7,500), mice treated with intrapleural Mz (1st generation CAR, no costimulatory signaling included) CAR T cells showed an unsustainable response in terms of tumor burden (Figure 2B) and median survival was 29 days longer than that in the P28z-treated controls (median survival, 45 vs. 16 days, P28z represents a xenoreactivity and alloreactivity control targeting the PSMA antigen) (Figure 2C). Mice treated with M28z CAR T cells had a more uniform reduction in tumor burden and survived longer (median survival, 64 days) than mice treated with first-generation CAR T cells; however, all mice treated with M28z CAR T cells eventually died of progressing tumor. We confirmed that tumor outgrowth was not caused by tumor antigen escape (recurring tumors in mice were found to be $MSLN^+$ by flow cytometric and histologic analysis; data not shown). In contrast, intrapleurally administered MBBz CAR T

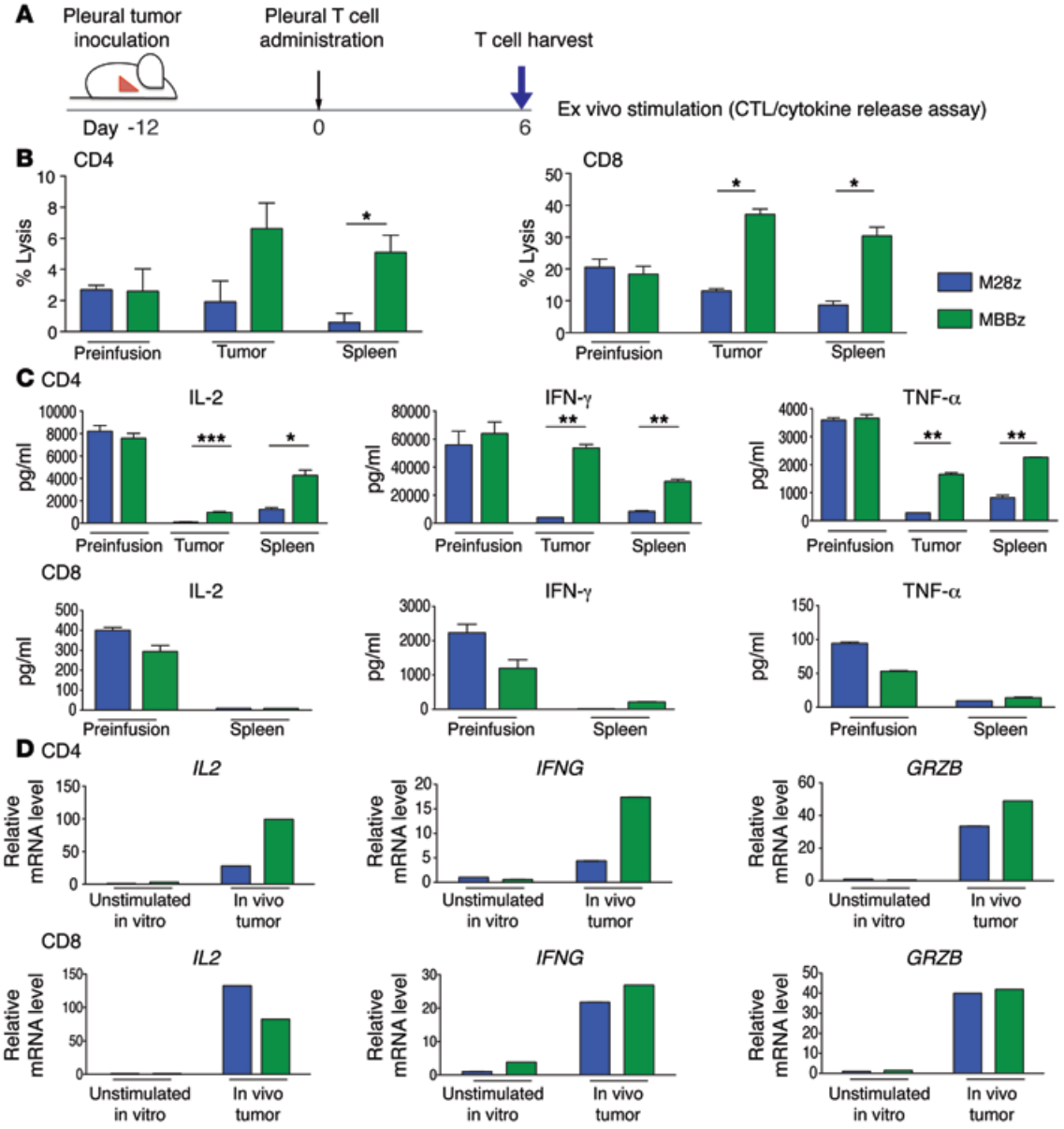

Figure 4. CAR T cells become exhausted following in vivo antigen exposure, although MBBz CAR T cells preferentially retain effector cytokine secretion and cytotoxicity. (**A**) Six days after intrapleural administration of CAR T cells, M28z and MBBz CAR T cells were isolated from the tumor and spleen and subjected to ex vivo antigen stimulation. (**B**) Chromium-release assay upon ex vivo stimulation demonstrates a decrease in M28z but persistent MBBz cytolytic function (E:T ratio, 5:1). (**C**) Cytokine secretion measurements demonstrate decreases in effector cytokine secretion by CAR T cells, although MBBz CAR T cells are better able to retain secretion. (**D**) RT-PCR measurements of *GRZB*, *IFNG*, and *IL2* expression by harvested CAR T cells correlate well with protein level measurements in panels **A** and **B**. Data represent the fold change relative to the mRNA expression of unstimulated M28z CAR T cell in vitro. Student's *t* tests were performed, and statistical significance was determined using the Sidak-Bonferonni correction for multiple comparisons. $^{*}P < 0.05$; $^{**}P < 0.01$; $^{***}P < 0.001$. Data represent the mean ± SEM of 3 individual wells per condition. Results are reproduced in 2 separate cohorts of mice used for each of the 2 experiments.

cells induced tumor eradication within 20 days of treatment, and the vast majority of mice (7 of 8) remained tumor free for more than 100 days (median survival was not reached by day 100).

MBBz surpasses M28z CAR T cells at low T cell doses. Improvements in CAR T cell efficacy afforded by costimulatory signaling are typically attributed to improvements in CAR T cell proliferation and/or persistence (2). As expected, M28z and MBBz CAR T cells achieved enhanced intratumoral T cell accumulation compared with Mz CAR T cells (9-fold greater for M28z, 12-fold greater for MBBz) (Figure 3A). Surprisingly, despite the differences in efficacy between M28z and MBBz CAR T cells, we observed similar numbers of tumor-infiltrating T cells between the 2 groups (Figure 3A). Furthermore, M28z and MBBz CAR T cells were equally persistent at long-term time points (Figure 3B). Equal accumulation and persistence were observed for both $CD4^+$ and $CD8^+$ T cell subsets (Supplemental Figure 2). Tumor tissue and spleen from M28z-treated mice that initially had a treatment response but then died of progressing tumor con-

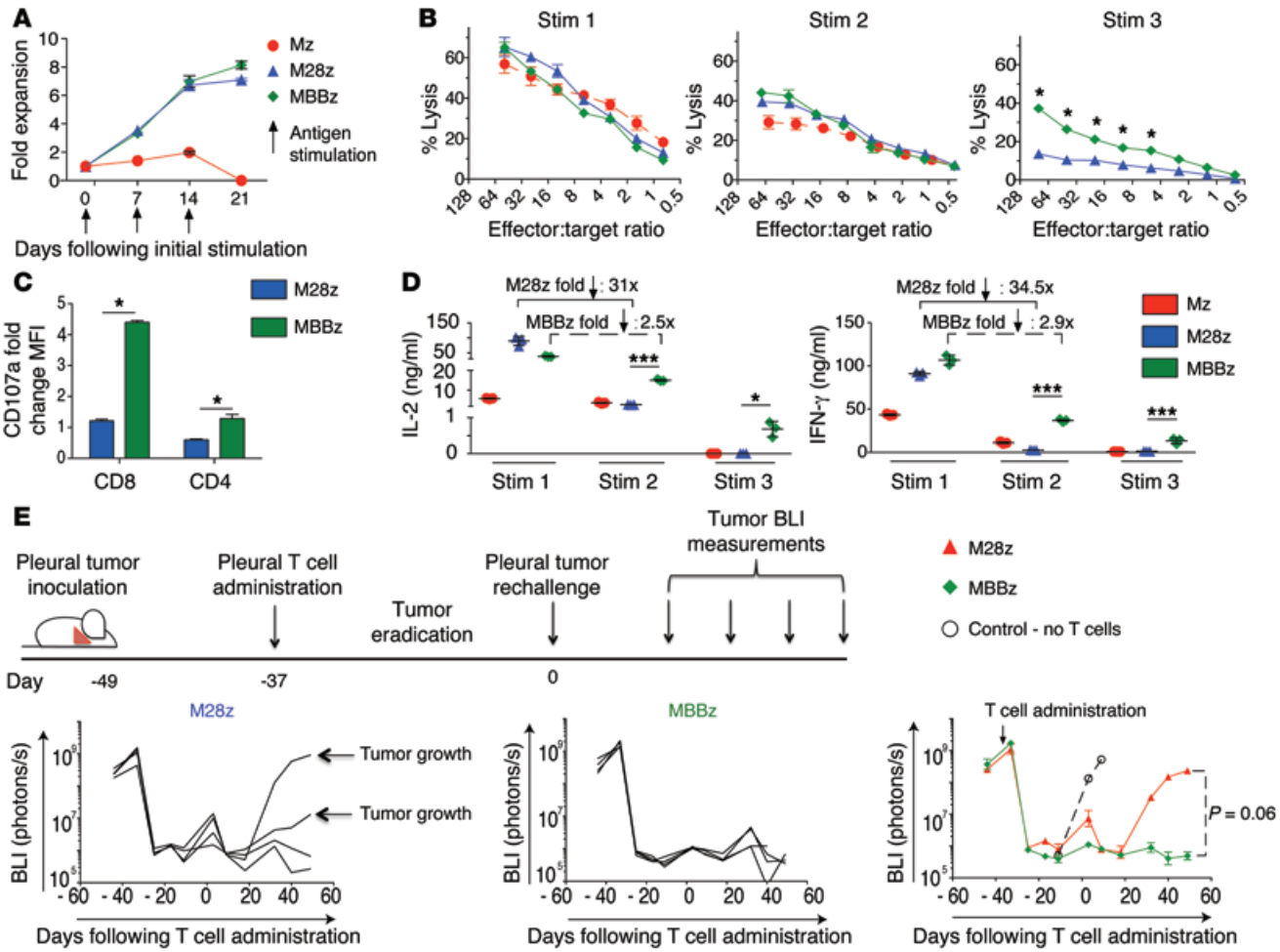

Figure 5. CAR T cells become exhausted upon repeated antigen stimulation in vitro, although MBBz CAR T cells preferentially retain effector cytokine secretion and cytotoxicity in vitro and upon tumor rechallenge in vivo. (**A**) Both M28z and MBBz CAR T cells retain proliferative capacity in vitro upon repeated antigen stimulation. T cells were also tested for cytotoxicity by chromium-release assay and for cytokine secretion by Luminex assay (**B**–**D**). (**B**) (Left) CAR T cells demonstrate equal killing at the first stimulation and loss of cytolytic function upon repeated antigen stimulation, although MBBz CAR T cells are better able to retain cytolytic function as measured by chromium-release assay. (**C**) Cytotoxic granule release as measured by CD107a expression correlates with chromium-release assay (**B**). Data represent the mean ± SD (triplicates) of the fold-change relative to the CD107a mean fluorescence intensity (MFI) of unstimulated $CD8^+$ CAR T cells. (**D**) Cytokine secretion measurements similarly demonstrate loss of CAR T cell effector function upon repeated antigen encounter; again, MBBz CAR T cells are better able to preserve their function. (**E**) Persisting MBBz CAR T cells demonstrate superior efficacy in vivo and eradicate $MSLN^+$ tumor cells following tumor rechallenge. Twenty-eight days after pleural tumor eradication (following a single dose of 1×10^5 CAR T cells), 1×10^6 $MSLN^+$ tumor cells were injected into the pleural cavity (tumor rechallenge). Control (white circle) represents mice without any previous injections of tumor or T cells. MBBz CAR T cells prevented tumor growth in all mice, whereas tumor growth and death were observed in 2 of 4 mice initially treated with M28z CAR T cells. Student's *t* tests were performed, and statistical significance was determined using the Sidak-Bonferonni correction. $^*P < 0.05$; $^{***}P < 0.001$. Data represent the mean ± SEM of 3 replicates or are plotted as individual points and are representative of at least 3 independent experiments.

tained circulating T cells as well as tumor-infiltrating T cells, including CAR-positive cells (Figure 3C). This finding demonstrates that the mere persistence of T cells that can effectively traffic to the tumor is not sufficient to eliminate tumor and that the T cell functional status within the tumor microenvironment may be the more critical determinant of clinical outcome. We therefore hypothesized that even costimulated T cells may become exhausted within tumor, especially at low T cell doses that correspond to low E:T ratios. Furthermore, MBBz CAR T cells, which were as persistent as M28z CAR T cells, may be better able to resist exhaustion and retain T cell effector function in order to eliminate a large tumor burden.

MSLN CAR T cells become exhausted following in vivo antigen exposure. To assess whether there is ongoing immunoinhibition of CAR T cells and to compare the relative abilities of M28z and MBBz CAR T cells to overcome tumor-mediated immunoinhibition, we injected 1×10^6 CAR T cells into the pleural cavities of MSTO $MSLN^+$ tumor–bearing mice, allowed sufficient time for T cell activation (confirmed by upregulation of the activation marker CD69; data not shown), and then performed ex vivo stimulation of harvested $CD4^+$ or $CD8^+$ CAR tumor-infiltrating or splenic T cells with $MSLN^+$ targets (schematic shown in Figure 4A). Uninjected in vitro resting T cells (preinfusion cells) were used to establish the baseline level of function (before antigen exposure). Compared

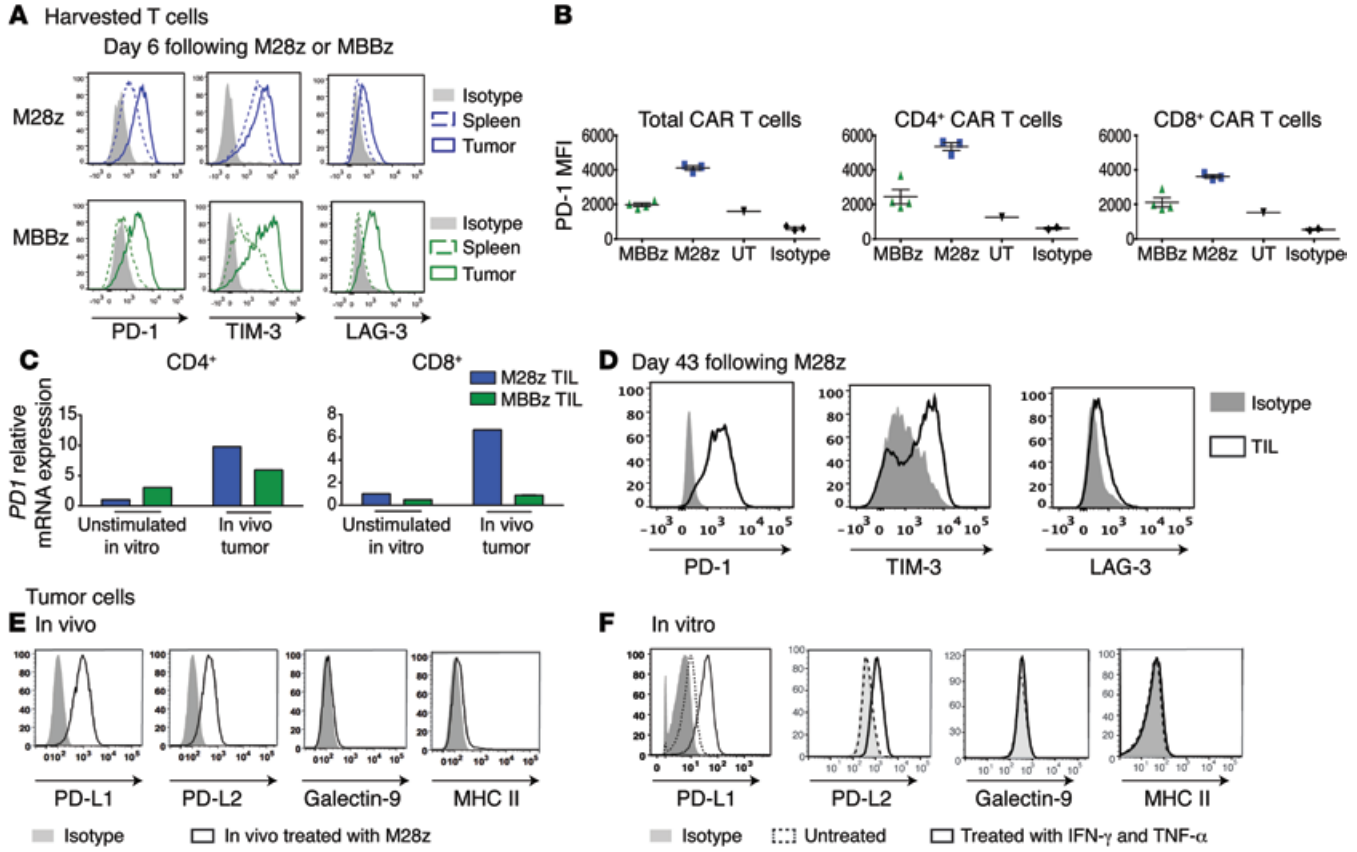

Figure 6. *PD1* receptor and its ligands are upregulated in vivo. (**A**) Tumor-infiltrating M28z and MBBz CAR T cells overexpressed inhibitory receptors 6 days after their administration. (**B**) MBBz CAR T cells express lower levels of PD-1 compared with M28z CAR T cells as shown by MFI of *PD1* receptor expression of tumor-infiltrating CAR T cells (TIL) 6 days after intrapleural administration. Unstransduced tumor-infiltrating T cells (UT) express a low baseline level of *PD1*. (**C**) Relative expression of *PD1* mRNA in CD4 and CD8 subsets of tumor-infiltrating CAR T cells 6 days after intrapleural administration. Data are represented as fold change relative to the *PD1* mRNA expression of unstimulated M28z CAR$^+$ T cells. (**D**) Tumor-infiltrating M28z CAR T cells isolated from progressing tumors express inhibitory receptors *PD1*, TIM-3, and LAG-3. (**E**) Single-cell tumor suspensions harvested from mice treated with M28z CAR T cells express high levels of PD-1–binding ligands. (**F**) In vitro–cultured mesothelioma tumor cells express the ligands (PD-L1, PD-L2) for the *PD1* receptor, and expression is further upregulated following incubation for 24 hours with IFN-γ and TNF-α. Data are representative of at least 2 to 3 independent experiments.

with resting M28z CD8$^+$ CAR T cells, T cells exposed to MSLN antigen in vivo had lower levels of cytolytic function (Figure 4B) (preinfusion cell lysis, 20.5%; tumor-infiltrating T cell lysis, 13.1%; splenic T cell lysis, 8.7%). In contrast, MBBz CAR T cells retained cytolytic function (preinfusion cell lysis, 18.3%; tumor-infiltrating T cell lysis, 37.2%; splenic T cell lysis, 22.2%). Sorted CD4$^+$ CAR T cells demonstrated a similar pattern of results. We also measured cytokine levels upon ex vivo stimulation of tumor-infiltrating and splenic CAR T cells and observed a decrease in Th1 cytokine secretion for CD4$^+$ M28z CAR T cells exposed in vivo to MSLN$^+$ antigen. CD4$^+$ MBBz CAR T cells also demonstrated a decrease in Th1 cytokine secretion, although these cells were better able to retain cytokine secretion when compared with M28z CAR T cells (Figure 4C). CD8$^+$ T cell supernatants contained significantly lower levels of cytokines compared with CD4$^+$ T cell supernatants (a finding previously observed in our model; ref. 8). CD8$^+$ T cells also had a decreased ability to secrete cytokines upon in vivo antigen exposure; CD8$^+$ MBBz CAR T cells preferentially retained their ability to secrete IFN-γ. We next assessed mRNA levels of T cells harvested from tumor and spleen on day 3 after administration and found that the in vivo expression levels of *GRZB*, *IL2*, and *IFNG* were mostly greater for CD4$^+$ and CD8$^+$ MBBz CAR T cells than for M28z CAR T cells, with the exception of IL-2 expression in the CD8$^+$ subset (Figure 4D).

MBBz CAR T cells show delayed exhaustion upon repeated antigen exposure. Having demonstrated inhibition of both the cytolytic function and effector cytokine secretion in costimulated CAR T cells exposed to antigen in vivo, we reasoned that repeated antigen stimulation may, similarly to that in models of chronic infection, play a role in T cell inhibition and that differing abilities to retain function upon repeated antigen encounter might explain enhanced efficacy of MBBz CAR T cells. We therefore tested Mz, M28z, and MBBz CAR T cells for their ability to withstand repeated antigen encounter in an in vitro model system, wherein cells were assessed for proliferation, cytolytic function, and cytokine secretion upon MSLN$^+$ antigen stimulation every 7 days. M28z and MBBz CAR T cells had similar abilities to expand upon serial MSLN$^+$ stimulation, expanding to levels 8- to 14-fold greater than those of Mz CAR T cells; they lost the ability to expand following the third stimulation (Figure 5A). Whereas lysis was equal among

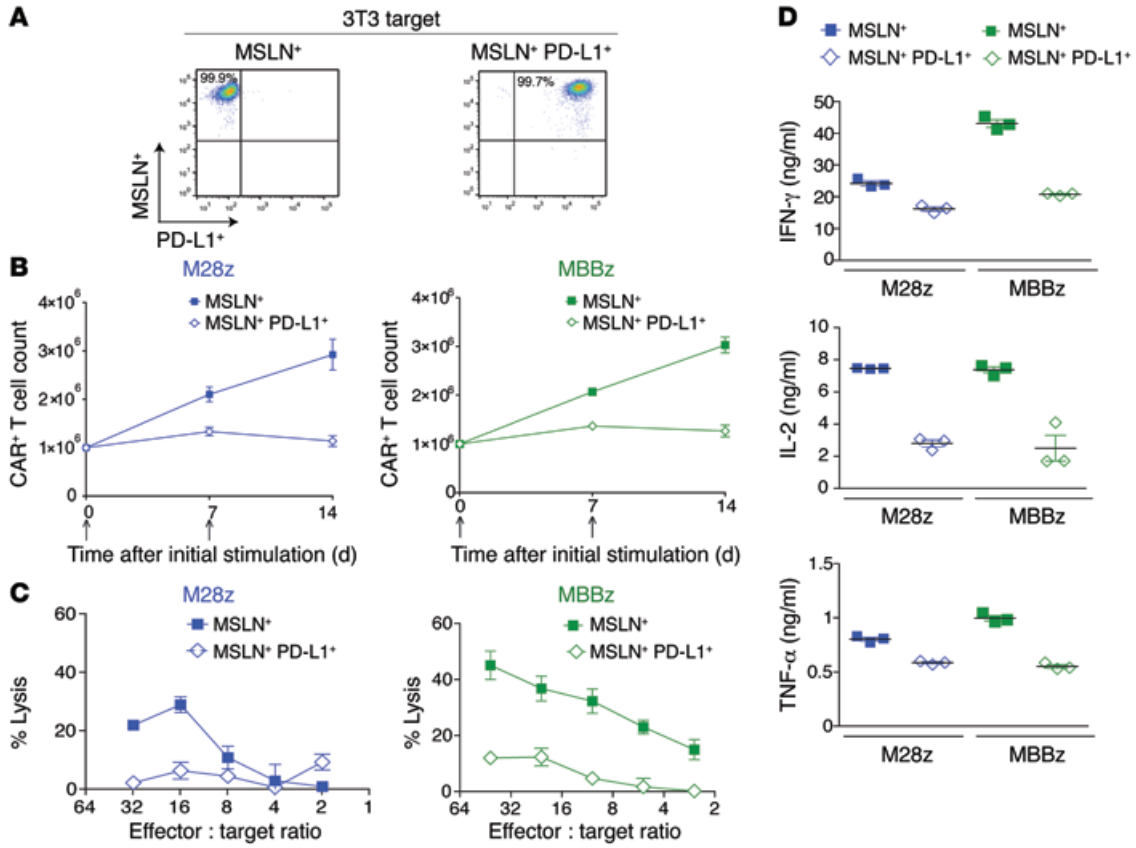

Figure 7. PD-L1 inhibits CAR T cell effector function. (**A**) 3T3 fibroblasts were transduced to either express MSLN alone (MSLN$^+$, left) or coexpress MSLN in addition to PD-L1 (MSLN$^+$ PD-L1$^+$, right). (**B**–**D**) M28z and MBBz CAR T cell effector functions were assessed after stimulation with 3T3 MSLN$^+$ or MSLN$^+$ PD-L1$^+$ targets. PD-L1 inhibits M28z and MBBz CAR T cell accumulation upon repeated antigen stimulation (**B**), cytolytic function following 2 stimulations with MSLN$^+$ PD-L1$^+$ tumor cells (**C**), and Th1 effector cytokine secretion upon the first stimulation (**D**). Data represent the mean ± SEM of 3 replicates or are plotted as individual points and are representative of at least 2 independent experiments.

the 3 T cell groups at the first stimulation, by the third stimulation, M28z lytic function was inhibited to a more pronounced level, MBBz CAR T cells were better able to retain lytic function at multiple E:T ratios (Figure 5B). Lytic function (as assessed by a degranulation assay measuring CD107a expression) at the third stimulation correlated with the results of chromium-release assays (Figure 5C). We next measured Th1 cytokine secretion and again noted similar levels between CD4$^+$ M28z and MBBz CAR T cells at the first stimulation as well as a successive decrease with each stimulation. As with cytotoxicity, MBBz CAR T cells preferentially retained cytokine secretion; cytokine concentrations decreased more than 30-fold for M28z and only around 2-fold for MBBz CAR T cells, when levels at the first and second stimulations were compared (Figure 5D). Similar results were observed with CD8$^+$ T cells. We then confirmed the differences in cytokine production by measuring intracellular levels of cytokines at the second stimulation (data not shown). Reverse-transcriptase PCR analysis of CAR T cells at the time of antigen stimulation revealed that MBBz CAR T cells expressed markers that correlate with lower levels of exhaustion and inhibition compared with M28z CAR T cells: MBBz CAR T cells expressed higher levels of *TBET* and EOMESODERMIN and lower levels of *PD1* and *FOXP3* (Supplemental Figure 3). We then sought to test the in vivo function of persisting CAR T cells that had already been exposed to tumor antigen, hypothesizing that MBBz CAR T cells would demonstrate enhanced function upon tumor rechallenge. Mice with established MSLN$^+$ pleural tumors were administered intrapleural M28z or MBBz CAR T cells (at a dose of 1×10^5, E:T ratio 1:3,000) to eradicate pleural tumor (Figure 5E). Twenty days after the initial T cell injection, tumor rechallenge was performed by injecting MSLN$^+$ tumor cells (1×10^6) into the pleural cavity of survivors; tumor burden was monitored using BLI. Persisting MBBz CAR T cells were better able to control tumor burden (4 of 4 MBBz-treated mice had a BLI signal at baseline levels vs. 2 of 4 M28z-treated mice) (Figure 5E). Furthermore, an independent experiment also demonstrated the ability of MBBz CAR T cells to eradicate MSLN$^+$ tumor in vivo following 3 tumor rechallenges (data not shown).

Tumor-cell PD-L1 inhibits MSLN CAR T cell effector functions. Having established that CAR T cells are inhibited in vitro and in vivo following repeated antigen encounter, we next sought to assess the role that inhibitory receptor and ligand pathways play in our model. Tumor-infiltrating T cells in M28z-treated mice with tumor progression showed high levels of expression of PD-1, T cell membrane protein 3 (TIM-3), and lymphocyte-activation gene 3 (LAG-3) (Figure 6A). Tumor-infiltrating MBBz CAR T cells harvested 6 days after administration demonstrated upregulation of inhibitory receptors as well, although they expressed significantly lower levels of PD-1 receptor at both the protein and the mRNA

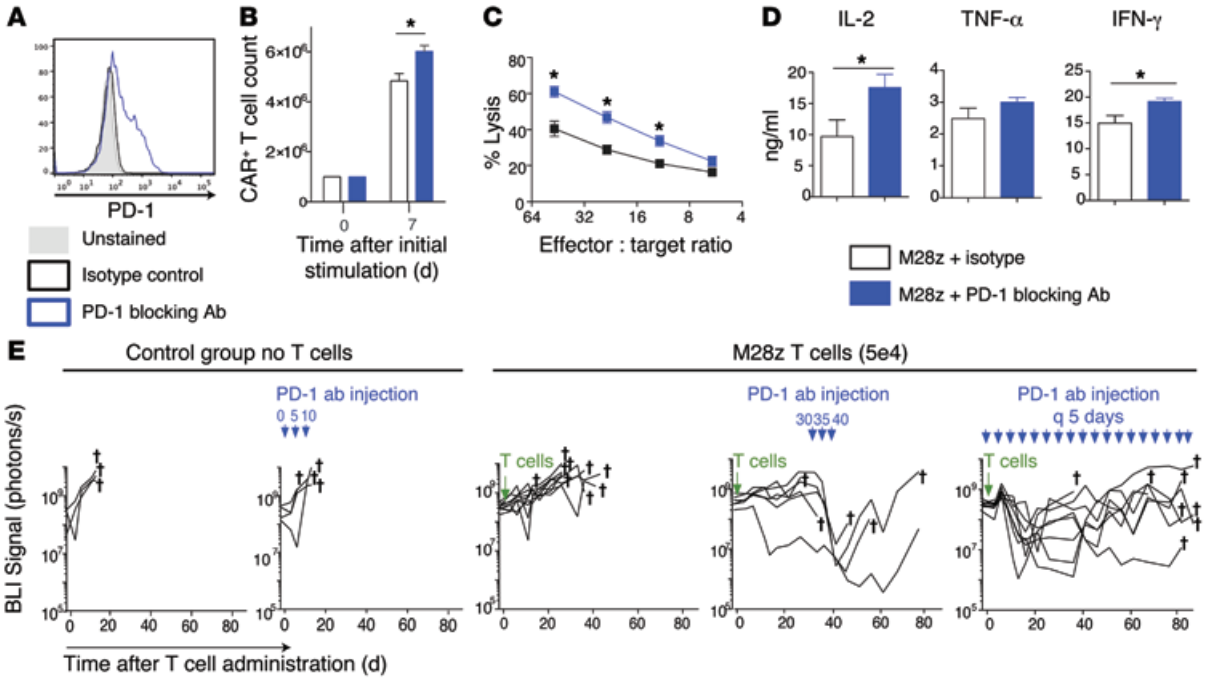

Figure 8. PD-1–blocking antibody restores the effector function of exhausted M28z CAR T cells in vitro and in vivo. (**A**) M28z CAR T cells were stained with the PD-1–blocking antibody used for functional assays. For in vitro experiments (**B**–**D**), M28z CAR T cells were stimulated with MSLN$^+$ tumor cells that had been treated with IFN-γ and TNF-α to upregulate PD-1 ligands. M28z CAR T cells treated with PD-1–blocking antibody (10 μg/ml) demonstrated a small enhancement in accumulation (**B**), an increase in cytolytic function upon the third stimulation (**C**), and enhanced effector cytokine secretion (**D**). Student's *t* tests were performed for statistical significance. Data represent the mean ± SEM of triplicates and are representative of 2–3 independent experiments. (**E**) Injection of PD-1–blocking antibody rescues M28z CAR T cells in vivo as shown by tumor BLI in a model treating established high tumor burdens with a single low dose of intrapleurally administered M28z CAR T cells. PD-1–blocking antibody (10 mg/kg) was injected intraperitoneally 3 times on days 30, 35, and 40 or continuously injected every 5 days from day 0 to day 85 following T cell injection. n = 6–9 mice per group. *$P < 0.05$.

level (Figure 6, A-C). CD4$^+$ T cells expressed higher levels of PD-1 compared with CD8$^+$ T cells (Figure 6, B and C). We also observed that a significant fraction of both M28z and MBBz CAR T cells coexpressed PD-1 and LAG-3 or PD-1 and TIM-3, suggesting that multiple inhibitory pathways could be functioning simultaneously (Supplemental Figure 4). We next assessed tumor-expressed ligands: PD-L1 and PD-L2 (ligands for PD-1), galectin-9 (ligand for TIM-3), and MHC class II (ligand for LAG-3). Only PD-1 ligands were expressed on pleural tumor cells harvested after intrapleural administration of M28z CAR T cells (Figure 6E). As reported elsewhere (18, 19), coculture of tumor cells with IFN-γ and TNF-α (at concentrations similar to those secreted by T cells, as shown in Figures 1 and 5) resulted in a similar level of upregulation of PD-L1 and PD-L2 expression on tumor cells (Figure 6F), reflecting an adaptation of tumor cells to resist immune attack (adaptive immunoresistance). The unique presence of expression of both PD-1 receptor and ligand in vivo suggests that this pathway may play a significant inhibitory role. As some studies have suggested that costimulation may be sufficient to overcome inhibition by PD-1 (35–37), we next assessed whether overexpressed PD-L1 can inhibit CAR T cell function in an in vitro model of PD-L1–mediated immunoinhibition (using 3T3 mouse fibroblasts transduced with either MSLN alone [MSLN$^+$] or both MSLN and PD-L1 [MSLN$^+$PD-L1$^+$]) (Figure 7A). In both M28z and MBBz CAR T cells, PD-L1 overexpression resulted in decreased accumulation upon successive stimulation (Figure 7B) and Th1 effector cytokine secretion (Figure 7D). Although tumor-cell lysis was not inhibited upon initial stimulation (data not shown), chromium-release assay performed with 3T3s as targets following 2 stimulations against MSTO MSLN$^+$ tumor cells demonstrated decreased lytic function in both M28z and MBBz CAR T cells (Figure 7C).

PD-1 antibody therapy rescues M28z CAR T cell function. As PD-1–blocking antibodies demonstrated beneficial effects in the treatment of a variety of malignancies including solid tumors, we next analyzed the ability of PD-1–blocking antibody to rescue exhausted CAR T cells in our model. For this purpose, we selected a PD-1–blocking antibody (clone EH12.2H7) that binds PD-1 receptors on M28z T cells (Figure 8A) and can (a) slightly enhance accumulation (Figure 8B); (b) improve cytotoxic activity (Figure 8C); and (c) improve cytokine secretion (Figure 8D). Next, we evaluated the ability of the PD-1–blocking antibody to rescue M28z CAR T cells in vivo. For this purpose, we injected a single, very low dose of M28z CAR T cells (5×10^4, E:T ratio, 1:6,000) into mice with large established tumor burdens with the objective of inducing the exhaustion of CAR T cells. In these conditions, CAR T cells were able to stabilize the tumor for 30 days (Figure 8E). At day 30, the PD-1 antibody was administered intraperitoneally at 10 mg/kg 3 times every 5 days (38–40). The marked decrease in tumor BLI following 3 doses of the antibody confirms that PD-1 is a relevant mechanism of CAR T cell inhibition in our model and suggests that PD-1 checkpoint blockade may be used to rescue exhausted M28z CAR T cells. However, tumor relapses observed following cessation of treatment suggest that efficacy is short lived and reliant upon repeated PD-1 antibody administration. We

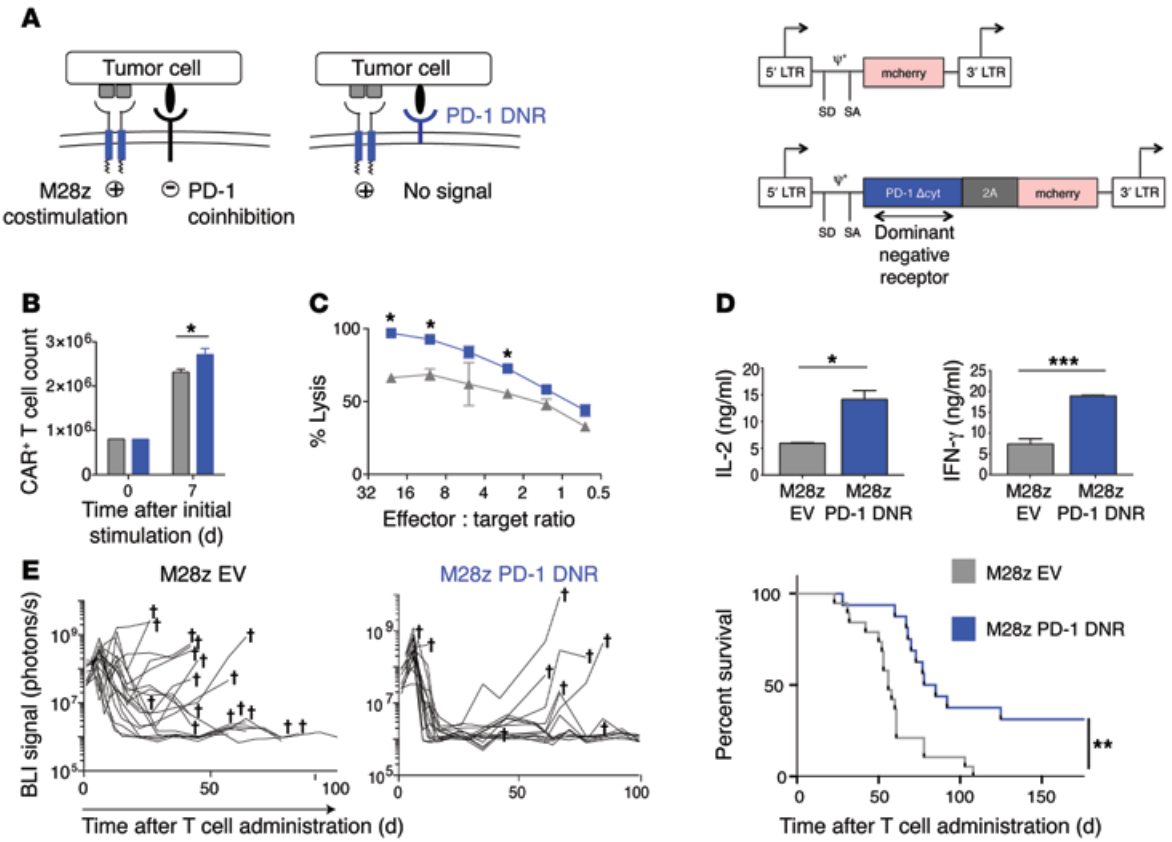

Figure 9. Cotransduction of a PD-1 DNR rescues M28z CAR T cells from PD-1 ligand–mediated inhibition in vitro and in vivo. (**A**) (Left) Schematic representations of CD28-costimulated T cells binding tumor ligand via the endogenous PD-1 receptor (transmitting a coinhibitory signal) or a cotransduced PD-1 DNR lacking an inhibitory signaling domain. (Right) For in vitro and in vivo experiments, M28z CAR T cells were cotransduced with either EV (SFG-mCherry) or PD-1 DNR (SFG-2A-PD-1 DNR). CAR T cells sorted for mCherry expression were then incubated for 24 hours with MSLN$^+$ tumor cells that had been treated with IFN-γ and TNF-α to upregulate PD-1 ligands. M28z PD-1 DNR CAR T cells demonstrated a small but statistically significant enhancement in accumulation (**B**), an enhanced cytolytic function, as measured by chromium-release assay upon the third stimulation with MSLN$^+$ PD-L1$^+$ tumor cells (**C**), and an increased expression of Th1 cytokine secretion (**D**). Student's *t* tests were performed, and statistical significance was determined using the Sidak-Bonferonni correction for multiple comparisons. $^*P < 0.05$; $^{**}P < 0.01$; $^{***}P < 0.001$. Data represent the mean ± SEM of triplicates and are representative of at least 3 independent experiments. (**E**) Tumor BLI (left) and Kaplan-Meier survival analysis (right) comparing the in vivo efficacy of a single dose of 5 × 10^4 M28z EV (n = 19; grey) or M28z PD-1 DNR (n = 16; blue) pleurally administered. Data shown are a combination of 2 independent experiments. Daggers indicate deaths. Median survival is shown in days following T cell administration. The survival curve was analyzed using the log-rank test (P = 0.001). The log-rank test for each independent experiment was significant at the $P < 0.05$ level; 2 experiments are combined for illustration.

have indeed observed in the same experiment that a second cycle of treatment restores the antitumor efficacy of CAR T cells (data not shown), thereby suggesting the necessity of multiple cycles of PD-1 antibody treatment for sustained efficacy. As shown in Figure 8E, multiple, long-term injections of the PD-1 antibody are able to control tumor burden but unable to eradicate the tumor.

Cell-intrinsic PD-1 resistance rescues M28z CAR T cell function in vivo. Since our goal was to provide CAR T cell–specific checkpoint blockade that was not reliant on repeated dosing of systemically administered antibodies, we focused on genetically engineered methods of overcoming immunoinhibition. We first constructed a PD-1 DNR that contained the extracellular ligand-binding domain of the receptor fused to a CD8 transmembrane domain. Since the PD-1 DNR lacks any signaling domain, we hypothesized that sufficiently overexpressed receptor would enhance T cell efficacy by saturating PD-1 ligands and thereby blocking signaling through the endogenous PD-1 receptor. We cotransduced M28z CAR T cells with either the PD-1 DNR linked by a P2A element to an mCherry reporter (PD-1 DNR) or an empty vector containing only the reporter (EV) (Figure 9A). M28z CAR T cells cotransduced with the PD-1 DNR had slight but statistically significant advantages in proliferative ability (Figure 9B) and enhanced cytotoxicity (Figure 9C) at multiple E:T ratios as well as augmented levels of IL-2 and IFN-γ secretion (Figure 9D). We next assessed whether intrapleural administration of M28z CAR T cells cotransduced with a genetically engineered PD-1 resistance would provide an in vivo advantage. Mice with established pleural MSLN$^+$-expressing tumors were administered a single intrapleural dose of 5 × 10^4 CAR$^+$ M28z EV or M28z PD-1 DNR T cells, and treatment response was monitored by tumor burden measurements (using serial BLI) and median survival. Mice treated with M28z PD-1 DNR T cells had significantly enhanced tumor burden control and prolonged median survival (Figure 9E); however, only some mice (7/16, 44%) had long-term tumor-free survival, suggesting that there are redundant mechanisms of immunoinhibition that must be overcome. To investigate an alternative genetic strategy for

overcoming PD-1–mediated immunoinhibition, we cotransduced M28z CAR T cells with vectors expressing PD-1–targeting shRNAs (Supplemental Figure 5A), which generated more than 60% PD-1 receptor knockdown at the protein level (Supplemental Figure 5B). In M28z CAR T cells, cotransduction with PD-1 shRNAs enhanced proliferative function upon $MSLN^+$ antigen stimulation (Supplemental Figure 5C), augmented cytotoxicity (Supplemental Figure 5D), and enhanced cytokine secretion upon stimulation with either mesothelioma cells or $MSLN^+PDL1^+$ 3T3 mouse fibroblasts (Supplemental Figure 5E) compared with cotransduction with an shRNA targeting a nonmammalian gene (M28z KanR). M28z PD-1 shRNA–transduced T cells did not achieve greater in vivo tumor rejection than M28z KanR T cells, but it is noteworthy that the level of knockdown was notably lower in vivo than in vitro. Thus, use of the PD1 DNR proved to be the more dependable strategy.

Discussion

We demonstrate here that CAR T cell therapy and PD-1 checkpoint blockade are a rational combination in a solid tumor model. To directly counteract PD-1–mediated inhibition, we used retroviral vectors to combine CAR-mediated costimulation with a PD-1 DNR. This combinatorial strategy (costimulation and checkpoint blockade) enhanced T cell function in the presence of tumor PD-L1 expression, resulting in long-term tumor-free survival following infusion of a single low dose of CAR T cells. Our study is relevant to the clinical practice of adoptive T cell therapy and immediately translational for the following reasons: (a) the costimulatory signaling domains tested — CD28 and 4-1BB — are the 2 costimulatory domains used in ongoing clinical trials (ClinicalTrials.gov NCT02414269, NCT02159716, NCT01583686); (b) our models of pleural mesothelioma recapitulate human disease and use large, clinically relevant tumor burdens that elucidate the relevance of T cell exhaustion (8, 15, 32, 33); and (c) our strategy of potentiating CAR T cells by genetically encoded checkpoint blockade uses human sequences that can be readily applied in the clinic (8, 30).

Our study demonstrates that human CAR T cells expressing second-generation CARs can be inhibited upon in vivo antigen exposure within the tumor microenvironment. Earlier studies have reported that agonistic costimulation alone can overcome some solid tumor–expressed inhibitory signaling, which may in part result from the use of immunosensitive in vivo models and the administration of high T cell doses that do not recapitulate the E:T ratios attained in patients with high tumor burdens (35–37). In the present experiments, high CAR T cell doses resulted in tumor eradication regardless of a CD28 or 4-1BB costimulatory domain. It is at the lower T cell doses (and resulting lower E:T ratios) that the effect of exhaustion became apparent. Our findings illustrate the importance of using clinically relevant in vivo models and evaluating the impact of T cell doses. The intrapleural T cell doses we used here (4×10^4 to 1×10^5 per mouse, equivalent to 1.2×10^5 to 3×10^6/kg) were markedly lower than those used in other mesothelioma xenografts studies (41, 42) and are comparable to doses used in current clinical trials for hematologic malignancies (3, 6) and solid tumors (43, 44). Our experimental design is thus particularly suited to characterizing the role of exhaustion in CAR T cell therapy.

Although both 4-1BB and CD28 costimulatory signaling enhanced T cell persistence to a similar degree, at lower E:T ratios, only treatment with 4-1BB–costimulated T cells eradicated tumors. 4-1BB–costimulated T cells, while still sensitive to tumor-mediated inhibition, were relatively resistant to decline in T cell cytolytic function and cytokine secretion both following in vivo antigen exposure and upon repeated antigen stimulation in vitro. The relative resistance of 4-1BB signaling to immunoinhibition is associated with a $PD\text{-}1^{lo}TBET^{hi}$, $eomesodermin^{hi}$ phenotype (45–49), which has been linked to less exhaustion and a more robust cytotoxic effector response in other tumor models and a model of chronic viral infection. This suggests that the criteria for selecting a particular costimulatory signaling strategy among the options available (i.e., 4-1BB, CD28, OX40L, 4-1BBL, CD27, etc.) should extend beyond T cell persistence to functional persistence. The selection of optimal costimulatory pathways will depend on the unique patterns of costimulatory and coinhibitory ligand expression by the tumor, the antigen expression level or density, the affinity of scFv for the tumor antigen, the distance of the tumor epitope from the membrane, and other variations in construct design (such as spacer and transmembrane domains) (2, 50–54). These variables — and not qualitative differences in signaling — may ultimately explain the variability seen in preclinical trials, which alternately conclude that 4-1BB or CD28 is superior, depending on the target antigen and tumor context.

The relatively higher expression of PD-1 in M28z CAR T cells led us to focus on CD28-stimulated CAR T cells. On the basis of this analysis, we pursued genetic strategies for counteracting PD-1 inhibitory signaling, such as generating a PD-1 DNR and shRNAs targeting PD-1. When expressed at sufficient levels, the PD-1 DNR competes with the endogenous PD-1 receptor for binding PD-1 ligands (PD-L1 and PD-L2). CD28-costimulated T cells cotransduced with PD-1 DNR demonstrated enhanced in vitro T cell functions and in vivo T cell efficacy, suggesting that PD-1 signaling is a significant mechanism by which tumor cells evade CAR T cells in our tumor model. Our findings point to the therapeutic promise of adoptively transferred T cells that are genetically engineered to resist tumor-mediated immune inhibition. A DNR that targets TGF-β has been validated in preclinical models and is currently being tested in clinical trials (55, 56).

Enhanced M28z efficacy was also demonstrated with coadministration of PD-1–targeting antibodies, further supporting PD-1 signaling as a significant mechanism of exhaustion in our model and posing an alternative therapeutic strategy for enhancing CAR T cell therapy. However, an obstacle that we observed in these preclinical studies and experienced in the clinic was the requirement for repeated antibody administration for optimal effect. This is in contrast to single administration of M28z PD-1 DNR required for enhanced efficacy. Since multiple parameters (i.e., antibody affinity and regimen, dose and pharmacokinetics, and tumor microenvironment) may influence the efficacy of the PD-1 antibody and PD-1 DNR, these experiments should not be used to infer or determine the superior efficacy of either strategy and, instead, should serve as further evidence of the importance of the PD-1 inhibitory pathway on CAR T cell exhaustion. While one may prefer the genetically engineered strategy for its efficacy, simplicity, and possible decreased risk profile, ultimately, both strat-

egies may be clinically used in concert — PD-1 antibodies used to disinhibit endogenous tumor-reactive T cells and the PD-1 DNR strategy used to boost adoptively transferred CAR T cell response.

Our proposed genetic strategy for coinhibitory blockade may overcome another obstacle limiting antibody therapy, the incidence of immune-related adverse events. Because it provides blockade of inhibitory pathways that is limited to a tumor-targeted T cell repertoire, adoptive transfer of PD-1–insensitive T cells may limit the autoimmunity that results from a more broadly applied antibody checkpoint blockade. Nonetheless, additional safety strategies are necessary to limit or prevent potential augmented autoimmunity of the genetically modified PD-1–insensitive T cells. Suicide gene "safety switch" systems already in use in clinical trials, such as iCaspase-9 (57), EGFR mutation (58), and herpes simplex virus thymidine kinase (59), which mediate T cell elimination after administration of a prodrug or antibody, can be used in PD-1 DNR CAR T cells. We, in fact, have incorporated the iCaspase-9 safety switch within the CAR in our ongoing phase I clinical trial of intrapleural administration of MSLN-targeted CAR T cells (ClinicalTrials.gov NCT02414269).

Our study is unique when compared with other reports characterizing CAR T cell exhaustion. Moon et al. characterize T cell hypofunction within an immunoresistant mesothelioma tumor (20); however, their characterization of inhibition rests on ex vivo experiments. In contrast, we confirm the presence of PD-1–mediated inhibition in vivo and demonstrate gene-engineered checkpoint blockade that can be employed in the clinic. Long et al. recently described CAR T cell exhaustion in a model of osteosarcoma (60) in that they describe an antigen-independent phenomenon that results from tonic signaling of aggregated CAR receptors. The T cells in their model became exhausted during ex vivo expansion, even prior to T cell transfer. Our results characterize a model of T cell exhaustion more akin to that developed in the chronic viral infection literature (61, 62) in which CAR T cell exhaustion is antigen dependent and results from exposure to repeated antigen encounters in an environment rich with inhibitory signaling.

Although we have identified one of the inhibitory mechanisms responsible for CAR T cell exhaustion and highlighted differences in the ability of costimulatory strategies to withstand immunoinhibition, we did not perform an exhaustive assessment of all inhibitory pathways potentially limiting T cell function. That a proportion of mice treated with M28z CAR T cells and PD-1 DNR or PD-1 antibody died of tumor progression suggests the action of other inhibitory mechanisms that remain to be explored. Similarly, that PD-L1 expression inhibits MBBz and M28z in vitro but does not inhibit MBBz efficiently in vivo may suggest that PD-L1 sensitivity is not the main/only factor distinguishing activities of MBBz and M28z CARs. Indeed, we observed that MBBz CAR T cells are associated with a more potent phenotype ($TBET^{hi}$, $eomesodermin^{hi}$, $FOXP3^{lo}$) and also expressed less immunosuppressive cytokines, such as IL-10 and TGF-β, compared with M28z (data not shown). The literature on chronic infection suggests the existence of other mechanisms of inhibition, both cell intrinsic and cell extrinsic, which have only started to be addressed in tumor-targeted T cell therapies (20, 63). Thus, resistance of MBBz to exhaustion in vivo is possibly a multifactorial resistance to multiple inhibitory mechanisms. Finally, a more complete analysis of the role played by inhibitory signaling would use an immunocompetent model that includes elements such as myeloid-derived suppressor cells and endogenous T cells that have been shown to play important roles in tumor immune evasion.

On the basis of the data presented herein, we have established the importance of tumor-mediated inhibition of human CAR T cell effector functions. By performing a comprehensive analysis of T cell effector functions, we established that costimulated CAR T cells that exhibit enhanced persistence are subject to inhibition upon repeated antigen encounter, both in vitro and within the tumor microenvironment. We have demonstrated the promise of CAR T cell therapy to counteract inhibitory signaling, as it offers the flexibility to engineer signaling domains that provide optimal costimulation and directly counteract inhibitory signals such as PD-1. In our ongoing clinical trial, we are evaluating the upregulation of inhibitory molecules on both the tumor and T cells within the tumor microenvironment. The knowledge acquired from this analysis in combination with the proof-of-principle preclinical experiments presented herein will be highly valuable in improving the efficacy of CAR T cell therapy for solid tumors. As with other solid malignancies, it may be that greater clinical benefit will be achieved by combined checkpoint blockade of multiple inhibitory pathways (e.g., PD-1, CTLA-4, LAG-3) (64). Ultimately, an ideal combination of costimulation with concurrent or adjuvant coinhibitory blockade will maximize CAR T cell potency; the chosen costimulatory and coinhibitory pathways may be tailored to the specific characteristics of tumor and patient.

Methods

General purpose. The purpose of this study was to characterize the mechanisms of tumor-mediated T cell inhibition and to enhance the efficacy of T cell immunotherapy for solid malignancies. We designed MSLN-targeted CARs that, when transduced into human T cells, provide tumor antigen recognition and antigen-specific effector function activation; we also designed signaling domains that provide costimulatory signaling and/or coinhibitory blockade. In vitro, we analyzed cytotoxicity, cytokine secretion, and T cell proliferation. In vivo experiments analyzed strategies for optimizing T cell therapy by use of a clinically relevant mouse model of orthotopic MPM. We used human cancer cells and human T cells to validate and facilitate the translation of our M28z CAR to the clinic, as we have previously demonstrated for CD19 (65) and PSMA (66) CAR T cells. Each experiment was performed multiple times using different donor T cells. To avoid confounding variables — such as differences due to transduction efficiencies and donor-related variability — we present data using a representative experiment, with sample replicates of more than 3.

Cell lines. MSTO-211H human pleural mesothelioma cells (ATCC) were retrovirally transduced to express GFP and ffLuc fusion protein (MSTO GFP-$ffLuc^+$). These cells were then transduced with the human MSLN variant 1 subcloned into an SFG retroviral vector to generate MSTO $MSLN^+$ GFP-$ffLuc^+$. Similarly, 3T3 murine fibroblasts (ATCC) were transduced with human MSLN variant 1 alone or with PD-L1 (OriGene cDNA subcloned into SFG vector) to generate 3T3 $MSLN^+$ and 3T3 $MSLN^+PD\text{-}L1^+$ cells.

γ-Retroviral vector construction and viral production. To generate MSLN-specific CARs, we engineered a cDNA encoding for a fully human scFv m912 specific for MSLN (provided by D. Dimitrov) (30)

linked to the CD8/CD3ζ, CD28/CD3ζ, or CD8/4-1BB/CD3ζ domain, as previously described (67). The control PSMA-specific CAR was generated similarly (66). For construction of the PD-1 DNR, we used commercial gene synthesis to encode the extracellular portion of the PD-1 receptor fused to the CD8 transmembrane and hinge domains. The CAR sequence was inserted into the SFG γ-retroviral vector (provided by I. Riviere, Memorial Sloan Kettering Cancer Center) and linked to a P2A sequence to induce coexpression of the LNGFR reporter (truncated low-affinity nerve growth factor receptor) or, in the case of the PD-1 DNR, the mCherry fluorescent protein reporter (68, 69). The CAR- and PD-1 DNR–encoding plasmids were then transfected into 293T H29 and 293VecRD114 packaging cell lines to produce the retrovirus, as previously described (70).

T cell isolation, gene transfer, and CD4/CD8 isolation. Peripheral blood mononuclear cells (PBMCs) were isolated by low-density centrifugation on Lymphoprep (Stem Cell Technology) and activated with phytohemagglutinin (2 ug/ml; Remel). Two days after isolation, PBMCs were transduced with 293VecRD114-produced retroviral particles encoding for CARs and PD-1 DNR and spinoculated for 1 hour at 1,800 *g* on plates coated with retronectin (15 μg/ml; r-Fibronectin, Takara). Transduced PBMCs were maintained in IL-2 (20 UI/ml; Novartis). Transduction efficiencies were determined by flow cytometric analysis. Pure populations of $CD4^+$ and $CD8^+$ CAR^+ T cells or mCherry-positive PD-1 DNR–expressing and mCherry-positive EV–expressing CAR^+ T cells were obtained by flow cytometric–based sorting.

Flow cytometry. Human MSLN expression was detected using a phycoerythrin-conjugated anti–human MSLN rat IgG2a (R&D Systems). Expression of costimulation or inhibitory proteins on tumor cells was analyzed using the following antibodies: 4-1BBL (PE, clone 5F4; BioLegend), MHC HLA-DR (PE, clone L203; R&D Systems), PD-L1 (APC, clone MIH1; eBioscience), PD-L2 (APC, clone MIH18; eBioscience), and galectin-9 (APC, clone 9M1-3; BioLegend). T cell phenotype and transduction efficiency were determined with monoclonal antibodies for CD3, CD4, CD8, and LNGFR. Expression of T cell inhibitory receptors was analyzed using PD-1 (APC, eBioJ105; eBioscience or EH12.2H7; Biolegend), TIM-3 (PE, clone 344823; R&D Systems), and LAG-3 (PE, clone C9B7W; BioLegend). Cell staining was analyzed using a BD LSRII flow cytometer and FlowJo analysis software (Tree Star Inc.).

T cell functional assays. The cytotoxicity of T cells transduced with a CAR or vector control was determined by standard ^{51}Cr-release assays (71). To perform the luciferase-activity assay, CAR^+ T cells and MSTO-211H cells expressing MSLN and ffLuc were incubated for 18 hours at different E:T ratios. Tumor-cell quantity was determined by BLI using IVIS 100/lumina II, after the addition of 100 μl of D-luciferin (15 mg/ml) per well, and was compared with the signal emitted by the tumor cells alone. CD107a and intracellular staining were performed after incubation of effector cells and irradiated MSTO-211H MSLN tumor cells for 18 hours in 24-well plates at a ratio of 5:1. For the CD107a assay, 5 μl of CD107a-PeCy7 antibody and GolgiStop were added at the time of stimulation.

Cytokine-release assays were performed by coculturing 5×10^3 to 1×10^6 T cells with target cells at a 1:1 to 5:1 ratio. After 6 to 24 hours of coculture, supernatants were collected. Cytokine levels were determined using a multiplex bead Human Cytokine Detection Kit in accordance with the manufacturer's instructions (Millipore).

To analyze the proliferation, CAR^+ T cells were stimulated on irradiated MSTO-211H cells or 3T3 cells expressing MSLN (and in the case of 3T3, with or without PD-L1) at an E:T ratio of 3:1 or 1:1 in triplicate. T cell numbers were counted 7 days following initial stimulation using a hemacytometer, with plotted numbers adjusted for CAR^+ percentage as determined by flow cytometry. Subsequently, T cells were restimulated under the same conditions and counted on day 14. To determine the rate of apoptosis for different CAR-transduced cells, T cells were collected at the time of seeding on day 0, day 7, and day 14 and stained for apoptosis markers (annexin V/7-AAD).

Orthotopic pleural mesothelioma animal model and ex vivo experiments. To develop the orthotopic mouse model of pleural mesothelioma, female NOD/SCIDγ mice (The Jackson Laboratory) aged 4 to 6 weeks were used. Mice were anesthetized using inhaled isoflurane and oxygen, with bupivacaine administered for analgesia. Direct intrapleural injection of 1×10^5 to 1×10^6 tumor cells in 200 μl of serum-free medium via a right thoracic incision was performed to establish orthotopic MPM tumors (8, 15, 32). In total, 4×10^4 to 1×10^5 transduced T cells (in 200 μl of serum-free medium) were adoptively transferred into tumor-bearing mice, into the thoracic cavity by direct intrapleural injection. PD-1–blocking antibody (clone EH12.2H7, Biolegend) was injected intraperitoneally at 10 mg/kg every 5 days. Tumor growth was monitored and quantified in vivo by BLI. BLI data were analyzed using Living Image software (version 2.6); BLI signal was reported as total flux (photons per second), which represents the average of ventral and dorsal flux. To analyze the functional capacity of CAR T cells ex vivo, tumor tissues and mouse spleen were processed and analyzed by FACS for phenotyping, or CAR^+ $CD4^+$ or $CD8^+$ T cells were sorted using a FACSAria sorter, then rested for 24 hours in RPMI with IL-2 (60 UI/ml), and ^{51}Cr-release and cytokine-release assays were performed as described above.

Quantitative real-time PCR. The mRNA from $CD4^+LNGFR^+$ or $CD8^+LNGFR^+$ sorted T cells was extracted and reverse transcribed into cDNA using μMACS One-Step cDNA Kit (MACS molecular, Miltenyi Biotech Inc.). Quantitative Real-Time PCR (RT-PCR) was performed with the TaqMan method using Applied Biosystems 7500 systems TaqMan Universal PCR Mastermix and TaqMan probes labeled with 6-carboxyfluorescein (FAM-MBG) and designed by Life Technologies: TBET (Hs00203436_m1); eomesodermin (Hs00172872_m1); granzyme B (Hs01554355_m1); IFN-γ (Hs00989291_m1); IL-2 (Hs00174114_m1); and PD-1 (Hs01550088_m1). The comparative Ct of the gene of interest was used and normalized to the β2m housekeeping gene using the following formula: ΔCt (sample) = Ct (gene of interest) – Ct (β2m). Then, the $2^{-\Delta\Delta Ct}$ method was used to analyze the relative fold change expression compared with the control condition and calculated as follows: $2^{-\Delta\Delta Ct} = 2^{\wedge}$-(ΔCt[sample] – ΔCt[control]).

Statistics. Data were analyzed using Prism (version 6.0; GraphPad Software) software and are presented as mean ± SEM, as stated in the figure legends. Results were analyzed using unpaired Student's *t* test (2-tailed), with the Sidak-Bonferroni correction used to correct for multiple comparisons when applicable. Survival curves were analyzed using the log-rank test. Statistical significance was defined as $P < 0.05$. All statistical analyses were performed with Prism software.

Study approval. The experimental procedures for the animal studies were approved by the Institutional Animal Care and Use Committee of Memorial Sloan Kettering Cancer Center.

Author contributions

PSA conceived and designed the study. LC, AM, JVV, and PSA conducted the experiments. PSA, LC, AM, and MS analyzed and interpreted the data. YF and DSD provided the scFv. PSA, LC, AM, MS, and DRJ wrote the manuscript. AM, PSA, LC, JVV, YF, DSD, DRJ, and MS reviewed and revised the manuscript. PSA, MS, and DRJ provided administrative, technical, or material support. PSA supervised the study.

Acknowledgments

The authors' laboratory work was supported in part by the Intramural Research Program of the Center for Cancer Research, National Cancer Institute, National Institutes of Health (NIH), grants from the NIH (P30 CA008748 and P50 CA086438-13), the US Department of Defense (PR101053, LC110202, and BC132124), Mr. William H. Goodwin and Alice Goodwin, the Commonwealth Foundation for Cancer Research, the Experimental Therapeutics Center, a Stand Up To Cancer — Cancer Research Institute Cancer Immunology Translational Cancer research grant (SU2C-AACR-DT1012), the DallePezze Foundation, the Derfner Foundation, the American College of Surgeons resident research scholarship, and the ETC Edythe Griffinger Fellowship Program. Stand Up To Cancer is a program of the Entertainment Industry Foundation administered by the American Association for Cancer Research. We thank David Sewell and Alex Torres of the Memorial Sloan Kettering Cancer Center (MSK) Thoracic Surgery Service for their editorial assistance. We also thank Nina Lampen and Laurent Schmitt for the electron microscopy image.

Address correspondence to: Prasad S. Adusumilli, Center for Cell Engineering, Thoracic Service, Department of Surgery, Memorial Sloan Kettering Cancer Center, 1275 York Avenue, New York, New York 10065, USA. Phone: 212.639.8093; E-mail: adusumip@mskcc.org.

1. Sadelain M, Rivière I, Brentjens R. Targeting tumours with genetically enhanced T lymphocytes. *Nat Rev Cancer*. 2003;3(1):35–45.
2. Sadelain M, Brentjens R, Rivière I. The basic principles of chimeric antigen receptor design. *Cancer Discov*. 2013;3(4):388–398.
3. Brentjens RJ, et al. CD19-targeted T cells rapidly induce molecular remissions in adults with chemotherapy-refractory acute lymphoblastic leukemia. *Sci Transl Med*. 2013;5(177):177ra38.
4. Brentjens RJ, et al. Safety and persistence of adoptively transferred autologous CD19-targeted T cells in patients with relapsed or chemotherapy refractory B-cell leukemias. *Blood*. 2011;118(18):4817–4828.
5. Davila ML, et al. Efficacy and toxicity management of 19-28z CAR T cell therapy in B cell acute lymphoblastic leukemia. *Sci Transl Med*. 2014;6(224):224ra25.
6. Grupp SA, et al. Chimeric antigen receptor-modified T cells for acute lymphoid leukemia. *N Engl J Med*. 2013;368(16):1509–1518.
7. Kalos M, et al. T cells with chimeric antigen receptors have potent antitumor effects and can establish memory in patients with advanced leukemia. *Sci Transl Med*. 2011;3(95):95ra73.
8. Adusumilli PS, et al. Regional delivery of mesothelin-targeted CAR T cell therapy generates potent and long-lasting CD4-dependent tumor immunity. *Sci Transl Med*. 2014;6(261):261ra151.
9. Argani P, et al. Mesothelin is overexpressed in the vast majority of ductal adenocarcinomas of the pancreas: identification of a new pancreatic cancer marker by serial analysis of gene expression (SAGE). *Clin Cancer Res*. 2001;7(12):3862–3868.
10. Frierson HF, et al. Large-scale molecular and tissue microarray analysis of mesothelin expression in common human carcinomas. *Hum Pathol*. 2003;34(6):605–609.
11. Gubbels JA, et al. Mesothelin-MUC16 binding is a high affinity, N-glycan dependent interaction that facilitates peritoneal metastasis of ovarian tumors. *Mol Cancer*. 2006;5(1):50.
12. Kachala SS, et al. Mesothelin overexpression is a marker of tumor aggressiveness and is associated with reduced recurrence-free and overall survival in early-stage lung adenocarcinoma. *Clin Cancer Res*. 2014;20(4):1020–1028.
13. Li M, et al. Mesothelin is a malignant factor and therapeutic vaccine target for pancreatic cancer. *Mol Cancer Ther*. 2008;7(2):286–296.
14. Rizk NP, et al. Tissue and serum mesothelin are potential markers of neoplastic progression in Barrett's associated esophageal adenocarcinoma. *Cancer Epidemiol Biomarkers Prev*. 2012;21(3):482–486.
15. Servais EL, et al. Mesothelin overexpression promotes mesothelioma cell invasion and MMP-9 secretion in an orthotopic mouse model and in epithelioid pleural mesothelioma patients. *Clin Cancer Res*. 2012;18(9):2478–2489.
16. Tozbikian G, et al. Mesothelin expression in triple negative breast carcinomas correlates significantly with basal-like phenotype, distant metastases and decreased survival. *PLoS ONE*. 2014;9(12):e114900.
17. Morello A, Sadelain M, Adusumilli PS. Mesothelin-targeted CARs: driving T cells to solid tumors. *Cancer Discov*. 2016;6(2):133–146.
18. McGray AJ, et al. Immunotherapy-induced CD8+ T cells instigate immune suppression in the tumor. *Mol Ther*. 2014;22(1):206–218.
19. Spranger S, et al. Up-regulation of PD-L1, IDO, and T(regs) in the melanoma tumor microenvironment is driven by CD8(+) T cells. *Sci Transl Med*. 2013;5(200):200ra116.
20. Moon EK, et al. Multifactorial T-cell hypofunction that is reversible can limit the efficacy of chimeric antigen receptor-transduced human T-cells in solid tumors. *Clin Cancer Res*. 2014;20(16):4262–4273.
21. Hodi FS, et al. Improved survival with ipilimumab in patients with metastatic melanoma. *N Engl J Med*. 2010;363(8):711–723.
22. Wolchok JD, et al. Nivolumab plus ipilimumab in advanced melanoma. *N Engl J Med*. 2013;369(2):122–133.
23. Topalian SL, et al. Safety, activity, and immune correlates of anti-PD-1 antibody in cancer. *N Engl J Med*. 2012;366(26):2443–2454.
24. Ji RR, et al. An immune-active tumor microenvironment favors clinical response to ipilimumab. *Cancer Immunol Immunother*. 2012;61(7):1019–1031.
25. Rizvi NA, et al. Cancer immunology. Mutational landscape determines sensitivity to PD-1 blockade in non-small cell lung cancer. *Science*. 2015;348(6230):124–128.
26. Hamid O, et al. A prospective phase II trial exploring the association between tumor microenvironment biomarkers and clinical activity of ipilimumab in advanced melanoma. *J Transl Med*. 2011;9:204.
27. John LB, et al. Anti-PD-1 antibody therapy potently enhances the eradication of established tumors by gene-modified T cells. *Clin Cancer Res*. 2013;19(20):5636–5646.
28. Strome SE, et al. B7-H1 blockade augments adoptive T-cell immunotherapy for squamous cell carcinoma. *Cancer Res*. 2003;63(19):6501–6505.
29. Mayor M, Yang N, Sterman D, Jones DR, Adusumilli PS. Immunotherapy for non-small cell lung cancer: current concepts and clinical trials. *Eur J Cardiothorac Surg*. 2016;49(5):1324–1333.
30. Feng Y, et al. A novel human monoclonal antibody that binds with high affinity to mesothelin-expressing cells and kills them by antibody-dependent cell-mediated cytotoxicity. *Mol Cancer Ther*. 2009;8(5):1113–1118.
31. Brentjens RJ, et al. Genetically targeted T cells eradicate systemic acute lymphoblastic leukemia xenografts. *Clin Cancer Res*. 2007;13(18 Pt 1):5426–5435.
32. Servais EL, Colovos C, Kachala SS, Adusumilli PS. Pre-clinical mouse models of primary and metastatic pleural cancers of the lung and breast and the use of bioluminescent imaging to monitor pleural tumor burden. *Curr Protoc Pharmacol*. 2011;Chapter 14:Unit14.21.
33. Servais EL, et al. An in vivo platform for tumor biomarker assessment. *PLoS ONE*. 2011;6(10):e26722.
34. Adusumilli PS, et al. Imaging and therapy of malignant pleural mesothelioma using replication-competent herpes simplex viruses. *J Gene Med*. 2006;8(5):603–615.
35. Carter L, et al. PD-1:PD-L inhibitory pathway affects both CD4(+) and CD8(+) T cells and is overcome by IL-2. *Eur J Immunol*. 2002;32(3):634–643.
36. Freeman GJ, et al. Engagement of the PD-1 immu-

noinhibitory receptor by a novel B7 family member leads to negative regulation of lymphocyte activation. *J Exp Med*. 2000;192(7):1027–1034.
37. Koehler H, Kofler D, Hombach A, Abken H. CD28 costimulation overcomes transforming growth factor-beta-mediated repression of proliferation of redirected human CD4+ and CD8+ T cells in an antitumor cell attack. *Cancer Res*. 2007;67(5):2265–2273.
38. Curran MA, Montalvo W, Yagita H, Allison JP. PD-1 and CTLA-4 combination blockade expands infiltrating T cells and reduces regulatory T and myeloid cells within B16 melanoma tumors. *Proc Natl Acad Sci USA*. 2010;107(9):4275–4280.
39. Moon EK, et al. Blockade of programmed death 1 augments the ability of human t cells engineered to target NY-ESO-1 to control tumor growth after adoptive transfer. *Clin Cancer Res*. 2016;22(2):436–447.
40. Seung E, Dudek TE, Allen TM, Freeman GJ, Luster AD, Tager AM. PD-1 blockade in chronically HIV-1-infected humanized mice suppresses viral loads. *PLoS ONE*. 2013;8(10):e77780.
41. Carpenito C, et al. Control of large, established tumor xenografts with genetically retargeted human T cells containing CD28 and CD137 domains. *Proc Natl Acad Sci USA*. 2009;106(9):3360–3365.
42. Zhao Y, et al. Multiple injections of electroporated autologous T cells expressing a chimeric antigen receptor mediate regression of human disseminated tumor. *Cancer Res*. 2010;70(22):9053–9061.
43. Louis CU, et al. Antitumor activity and long-term fate of chimeric antigen receptor-positive T cells in patients with neuroblastoma. *Blood*. 2011;118(23):6050–6056.
44. Beatty GL, et al. Mesothelin-specific chimeric antigen receptor mRNA-engineered T cells induce anti-tumor activity in solid malignancies. *Cancer Immunol Res*. 2014;2(2):112–120.
45. Curran MA, et al. Systemic 4-1BB activation induces a novel T cell phenotype driven by high expression of Eomesodermin. *J Exp Med*. 2013;210(4):743–755.
46. Hirschhorn-Cymerman D, et al. Induction of tumoricidal function in CD4+ T cells is associated with concomitant memory and terminally differentiated phenotype. *J Exp Med*. 2012;209(11):2113–2126.
47. Song C, Sadashivaiah K, Furusawa A, Davila E, Tamada K, Banerjee A. Eomesodermin is required for antitumor immunity mediated by 4-1BB-agonist immunotherapy. *Oncoimmunology*. 2014;3(1):e27680.
48. Schietinger A, Delrow JJ, Basom RS, Blattman JN, Greenberg PD. Rescued tolerant CD8 T cells are preprogrammed to reestablish the tolerant state. *Science*. 2012;335(6069):723–727.
49. Kao C, et al. Transcription factor T-bet represses expression of the inhibitory receptor PD-1 and sustains virus-specific CD8+ T cell responses during chronic infection. *Nat Immunol*. 2011;12(7):663–671.
50. James SE, et al. Antigen sensitivity of CD22-specific chimeric TCR is modulated by target epitope distance from the cell membrane. *J Immunol*. 2008;180(10):7028–7038.
51. James SE, et al. Mathematical modeling of chimeric TCR triggering predicts the magnitude of target lysis and its impairment by TCR downmodulation. *J Immunol*. 2010;184(8):4284–4294.
52. Watanabe K, et al. Target antigen density governs the efficacy of anti-CD20-CD28-CD3 ζ chimeric antigen receptor-modified effector CD8+ T cells. *J Immunol*. 2015;194(3):911–920.
53. Hombach AA, Schildgen V, Heuser C, Finnern R, Gilham DE, Abken H. T cell activation by antibody-like immunoreceptors: the position of the binding epitope within the target molecule determines the efficiency of activation of redirected T cells. *J Immunol*. 2007;178(7):4650–4657.
54. Chmielewski M, Hombach A, Heuser C, Adams GP, Abken H. T cell activation by antibody-like immunoreceptors: increase in affinity of the single-chain fragment domain above threshold does not increase T cell activation against antigen-positive target cells but decreases selectivity. *J Immunol*. 2004;173(12):7647–7653.
55. Foster AE, et al. Antitumor activity of EBV-specific T lymphocytes transduced with a dominant negative TGF-beta receptor. *J Immunother*. 2008;31(5):500–505.
56. Bollard CM, et al. Adapting a transforming growth factor beta-related tumor protection strategy to enhance antitumor immunity. *Blood*. 2002;99(9):3179–3187.
57. Di Stasi A, et al. Inducible apoptosis as a safety switch for adoptive cell therapy. *N Engl J Med*. 2011;365(18):1673–1683.
58. Wang X, et al. A transgene-encoded cell surface polypeptide for selection, in vivo tracking, and ablation of engineered cells. *Blood*. 2011;118(5):1255–1263.
59. Ciceri F, et al. Infusion of suicide-gene-engineered donor lymphocytes after family haploidentical haemopoietic stem-cell transplantation for leukaemia (the TK007 trial): a non-randomised phase I-II study. *Lancet Oncol*. 2009;10(5):489–500.
60. Long AH, et al. 4-1BB costimulation ameliorates T cell exhaustion induced by tonic signaling of chimeric antigen receptors. *Nat Med*. 2015;21(6):581–590.
61. Barber DL, et al. Restoring function in exhausted CD8 T cells during chronic viral infection. *Nature*. 2006;439(7077):682–687.
62. Mueller SN, Ahmed R. High antigen levels are the cause of T cell exhaustion during chronic viral infection. *Proc Natl Acad Sci USA*. 2009;106(21):8623–8628.
63. Riese MJ, et al. Enhanced effector responses in activated CD8+ T cells deficient in diacylglycerol kinases. *Cancer Res*. 2013;73(12):3566–3577.
64. Hellmann MD, Friedman CF, Wolchok JD. Combinatorial Cancer Immunotherapies. *Adv Immunol*. 2016;130:251–277.
65. Brentjens RJ, et al. Eradication of systemic B-cell tumors by genetically targeted human T lymphocytes co-stimulated by CD80 and interleukin-15. *Nat Med*. 2003;9(3):279–286.
66. Gade TP, et al. Targeted elimination of prostate cancer by genetically directed human T lymphocytes. *Cancer Res*. 2005;65(19):9080–9088.
67. Zhong XS, Matsushita M, Plotkin J, Riviere I, Sadelain M. Chimeric antigen receptors combining 4-1BB and CD28 signaling domains augment PI3kinase/AKT/Bcl-XL activation and CD8+ T cell-mediated tumor eradication. *Mol Ther*. 2010;18(2):413–420.
68. Markley JC, Sadelain M. IL-7 and IL-21 are superior to IL-2 and IL-15 in promoting human T cell-mediated rejection of systemic lymphoma in immunodeficient mice. *Blood*. 2010;115(17):3508–3519.
69. Papapetrou EP, et al. Stoichiometric and temporal requirements of Oct4, Sox2, Klf4, and c-Myc expression for efficient human iPSC induction and differentiation. *Proc Natl Acad Sci USA*. 2009;106(31):12759–12764.
70. Hollyman D, et al. Manufacturing validation of biologically functional T cells targeted to CD19 antigen for autologous adoptive cell therapy. *J Immunother*. 2009;32(2):169–180.
71. McCoy JL, Herberman RB, Rosenberg EB, Donnelly FC, Levine PH, Alford C. 51 Chromium-release assay for cell-mediated cytotoxicity of human leukemia and lymphoid tissue-culture cells. *Natl Cancer Inst Monogr*. 1973;37:59–67.